Performance of Optimal Feedback Controller for Unified Power Quality Conditioner

P. Snigdha Tejaswi[1*],
PG Scholar, Department of EEE,
GITAM University, Vishakapatnam, India

S. Srinivasa Rao[2]
Assistant Professor, Department of EEE,
GITAM University, Vishakapatnam, India

***Abstract--* Power Quality (PQ) is a problem that is collectively significant to electricity consumers at all levels of usage. Custom power devices have developed, which are applicable to distribution system for improving the reliability and Power Quality. The unified power quality conditioner (UPQC) is flexible custom power device that will work as both DSTATCOM and DVR and used for balanced sinusoidal load voltages and source currents under distorted and unbalanced three-phase supply in power distribution system. Linear quadratic regulator (LQR) control technique is used to coordinate the operation of the series and shunt VSIs of the UPQC. LQR coordination ensures that the UPQC operates satisfactorily without depleting the limited energy of the dc link capacitors. But LQR may not be able to lead satisfactory performance under other operating conditions and adversely affect the performance of shunt compensation scheme. This paper implements optimal feedback controller i.e., particle swarm optimization based feedback controller for UPQC because feedback controller has optimal performance in several operating circumstances and is robust to parametric uncertainties compared to the conventional feedback controllers i.e., linear quadratic regulator.**

Keywords-- Unified power quality conditioner (UPQC), State feedback control, Linear Quadratic Regulator (LQR), Particle Swarm Optimization (PSO) technique, instantaneous symmetrical components, Total Harmonic Distortion (THD)

I. INTRODUCTION

By the advancement of power electronic devices like continuous adjustable speed drives power supply, etc., in distribution system, power quality problems such as harmonics, voltage fluctuations and flickering are increasing. Lightening, switching of capacitor banks and network faults may cause various power quality problems such as voltage swell/sag. Along with these the usage of power electronic equipment's, unbalanced and nonlinear loads by the consumers has degraded the PQ in the power distribution network. But on the other hand, telecoms, information technology, semiconductor manufacturing industries etc., are relatively sensitive to power quality problems and need high quality of electric power. Various schemes for the mitigation of the PQ issues have evolved in the literature. The most traditional scheme involves the use of passive filters. The passive filters consist of capacitors which are tuned at a particular frequency. Although they are simple in operation, they have many limitations.

Under these circumstances, in order to overcome the problems with passive filters and to improve the PQ in power distribution system, Active Power filters (APF) are proposed. The application of APFs in power distribution system is referred as Custom Power Devices. Distribution Static Compensator DSTATCOM is a shunt connected custom power device. It alleviates the current related power quality problems in the distribution system. Dynamic Voltage Restorer (DVR) is a series compensated custom power device. The purpose of the DVR is to protect the sensitive loads from voltage sag/swell, interruptions and harmonics on supply side voltage. UPQC fulfills different purposes like, keeping a sinusoidal nominal voltage at the bus, maintain voltage when there are voltage swells and sags in the system, removing harmonics in the load voltage and source currents, compensating reactive power, load balancing, power factor correction and negative sequence current. There are different algorithms and switching control schemes available in the literature to attain the abovementioned objectives[1]-[6].

Various control algorithms have been proposed to tackle the PQ problems using UPQC[5]-[9]. Most of the design methodologies available so far in the literature have not considered some of the important aspects, such as variations in the system parameters, including load impedance, feeder impedance and harmonics in load currents or source voltage. Due to present uncertainties in the system, the problem of compensating the system becomes more complicated which adversely effects the satisfactory operation of the UPQC.

In this paper, in order to make the feedback controller more robust to parametric variations, a new method, utilizing particle swarm optimization (PSO) has been proposed for designing the feedback controller. The state feedback controller, designed by using the proposed method, is robust to parametric uncertainties. In this paper, the efficiency of the proposed control technique is demonstrated through detailed simulation. The performance of the proposed feedback controller of UPQC is also compared with the conventional LQR-based feedback controller.

II. STRUCTURE OF UPQC

The proposed topology of UPQC connected to three phase, four wire distribution system is shown in Fig.1. It consists of six H-bridge inverters and six interfacing transformers to realize the two inverter circuits as shown. This topology enables the independent control of each leg of both the series and shunt inverters. The output will have very low harmonic content (i.e., it will have smooth tracking performance when the H bridge inverter is used). Use of this topology avoids the capacitor voltage balancing, since only one capacitor is used and the rating of the dc link is less compared to the other topologies. The common DC storage capacitor C_{dc} supports the series and shunt inverters. This topology enables injecting the filter currents and filter voltages independent of each other. The AC capacitor connected at the output of the transformer provides a path for switching frequency harmonics. The transformers provide isolation and prevent the DC capacitor from being shorted due to the operation of various switches

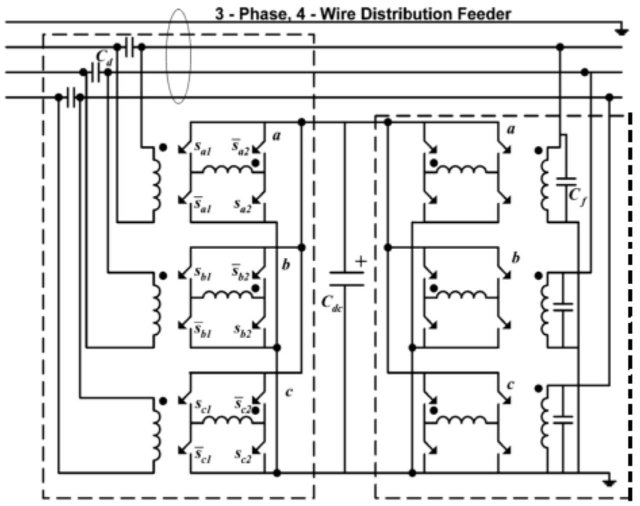

Series inverter with Capacitor filter

shunt inverter with capacitor filter

Fig.1. Topology of UPQC

The UPQC compensated distribution system is shown in Fig.2. The load is unbalanced and nonlinear. We denote the load voltage at this point of common coupling (PCC) by V_l the source voltage by V_s, and the terminal by V_t . The resistance R_s and the inductor L_s denote the feeder impedance. UPQC contains a series voltage source V_d, which is injected in such a way that the load voltage V_l is a balanced sinusoid irrespective of unbalance and distortion in the terminal voltage. Similarly, the UPQC has a shunt current source which injects current i_f so that the source current i_s is sinusoid irrespective of distortion in the load currents. Therefore, the main objective of the UPQC is to provide distortion-free voltage at the load and drawing a pure sinusoidal current from the supply.

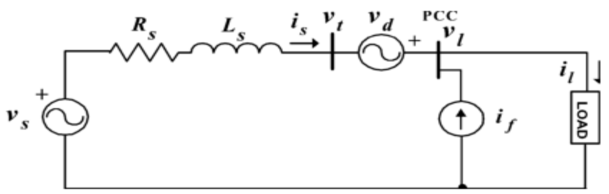

Fig.2. UPQC compensated distribution system

III. STATE FEEDBACK CONTROL OF UPQC

To derive state space modeling of the system done with the help of equivalent circuit of UPQC shown in Fig.3 The linear load is denoted by R_l and L_l. The term i_h represents the nonlinear load current. The parameters L_d and C_d represents the LC filter across series inverter. The resistors R_d and R_f represents the inverter losses in the series and shunt inverter, respectively. The inductances L_t and L_f represent the leakage inductance of the transformer connected in series and shunt, respectively. The shunt filter capacitor is represented by C_f. The voltage V_d is the series injected voltage and v_{sd} is the voltage across the capacitor C_d. Both the series and shunt inverters are supplied by common capacitor and the voltage across it denoted by V_{dc}. Voltage at the load terminal is the voltage across the filter capacitor C_f. The switched voltages across the series and shunt inverter output terminals are represented by $V_{dc}u_1$ and $V_{dc}u_2$, respectively

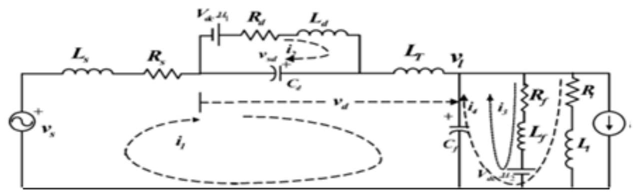

Fig.3. Single phase equivalent circuit of UPQC compensated system

The state-space model of the system is derived by six local variables (i.e., four loop currents and two capacitor voltages). Now the state vector is defined as given in the following

$$x^T = [i_1\ i_2\ i_3\ i_4\ v_{sd}\ v_l\,] \tag{1}$$

The circuit shown in Fig.3. contains four forcing functions. They are source voltage v_s, the nonlinear load current i_h and switching variables u_1 and u_2. Replace variables u_1 and u_2 by the continuous time variables u_{c1} and u_{c2} respectively and define the control vector as below.

$$u^T = [u_{c1}\ u_{c2}] \tag{2}$$

The state-space equation of the circuit can then be written as

$$\dot{x} = Ax + B_1 u + B_2 v_s + B_3 i_h \tag{3}$$

Where,

$$A = \begin{bmatrix} -R_s/(L_s+L_T) & 0 & 0 & 0 & 1/(L_s+L_T) & -1/(L_s+L_T) \\ 0 & -R_{se}/L_{se} & 0 & 0 & -1/L_{se} & 0 \\ 0 & 0 & -R_f/L_f & 0 & 0 & 1/L_f \\ 0 & 0 & 0 & -R_l/L_l & 0 & 1/L_l \\ 1/C_d & -1/C_d & 0 & 0 & 0 & 0 \\ 1/C_f & 0 & -1/C_f & -1/C_f & 0 & 0 \end{bmatrix}$$

$$B_1 = \begin{bmatrix} 0 & 0 \\ V_{dc}/L_d & 0 \\ 0 & -V_{dc}/L_f \\ 0 & 0 \\ 0 & 0 \\ 0 & 0 \end{bmatrix}$$

$$B_2 = \begin{bmatrix} 1/(L_s + L_T) \\ 0 \\ 0 \\ 0 \\ 0 \\ 0 \end{bmatrix} \quad B_3 = \begin{bmatrix} 0 \\ 0 \\ 0 \\ 0 \\ 0 \\ -1/C_f \end{bmatrix}$$

The system represented by the state-space model in Fig.3. Contains feeder impedance, load impedance and compensator parameters. Since all these state variables defined in the equation (3) are not measurable, the state variables can be written as network parameters as follows

$$\left.\begin{aligned} i_s &= i_1 \\ i_l &= i_4 \\ i_f &= i_4 - i_1 \\ i_{cf} &= i_1 - i_3 - i_4 \\ i_{cd} &= i_2 - i_1 \end{aligned}\right\} \qquad (4)$$

Where i_{cf} and i_{cd} are the charging currents of the capacitors C_f and C_d respectively. A transformed state vector Z which relates to the state vector x with the network parameters using (4) can be written as,

$$z = \begin{bmatrix} i_f \\ i_{cf} \\ v_l \\ i_{cd} \\ v_{sd} \\ i_l \end{bmatrix} = \begin{bmatrix} -1 & 0 & 0 & 1 & 0 & 0 \\ 1 & 0 & -1 & -1 & 0 & 0 \\ 0 & 0 & 0 & 0 & 0 & 1 \\ -1 & 1 & 0 & 0 & 0 & 0 \\ 0 & 0 & 0 & 0 & 1 & 0 \\ 0 & 0 & 0 & 1 & 0 & 1 \end{bmatrix} x = Px \qquad (5)$$

The state-space equation (1) is transformed by using (5) as,

$$\begin{aligned} \dot{z} &= PAP^{-1}z + PB_1u + PB_2v_s + PB_3i_h \\ &= \Lambda z + \Gamma_1 u + \Gamma_2 v_s + \Gamma_3 i_h \end{aligned} \qquad (6)$$

Assuming that we have full control over u, the control input is given by

$$u = -K(z - z_{ref}) \qquad (7)$$

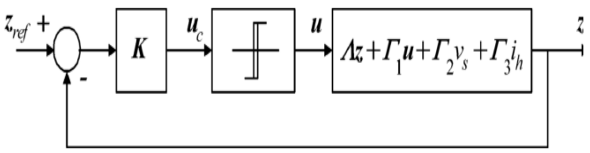

Fig.4. Switching control of the UPQC in the forward path

Where z_{ref} the desired state is vector and K is feedback gain matrix which is conventionally computed by the LQR method[5]-[7]. The block diagram of switching control is given in Fig.4. For the state feedback controller to perform satisfactorily, z_{ref} the reference for the transformed z should be chosen judiciously by obeying the network laws. The reference vector is computed as, $Z^{\Gamma}_{ref} = [i_f^{ref}\ i_{cf}^{ref}\ v_l^{ref}\ i_{cd}^{ref}\ v_{sd}^{ref}\ i_l^{ref}]$, Γ where represents the transpose of the matrix. The reference quantities generation is explained in detailed in the next section.

IV. REFERENCE QUANTITIES GENERATION AND SWITCHING CONTROL

The reference generation for UPQC is based on the half cycle averaging of current and voltage waveforms. The generation of reference voltage and current quantities under various conditions is discussed below. To extract the sinusoidal steady state quantities, we use instantaneous symmetrical component theory[12] and [13]. When the source voltages and load currents are unbalanced the reference quantities are given in below equations (8). Here the subscripts 0, +, - represent the zero, positive and negative sequence components respectively. The suffix 'ref' represents the reference quantity.

$$\left.\begin{aligned} I^{ref}_{fabc} &= \begin{bmatrix} I^{ref}_{fa} \\ I^{ref}_{fb} \\ I^{ref}_{fc} \end{bmatrix} = M^{-1}\begin{bmatrix} I^{ref}_{f0} \\ I^{ref}_{f1} \\ I^{ref}_{f2} \end{bmatrix} = \begin{bmatrix} I_{l0} \\ \dfrac{\beta|q_{lav}|}{|V_{l1}|} \\ I_{l2} \end{bmatrix} \\ I^{ref}_s &= I_{l1} - I^{ref}_{f1} \\ I^{ref}_s &= I_{l1} - I^{ref}_{f1} \\ V^{ref}_{sdabc} &= \begin{bmatrix} V^{ref}_{sda} \\ V^{ref}_{sdb} \\ V^{ref}_{sdc} \end{bmatrix} = M^{-1}\begin{bmatrix} V^{ref}_{sd0} \\ V^{ref}_{sd1} \\ V^{ref}_{sd2} \end{bmatrix} = M^{-1}\begin{bmatrix} -V_{t0} \\ V^{ref}_{d1} + \omega L_T I^{ref}_s e^{j90^0} \\ -V_{t2} \end{bmatrix} \\ I^{ref}_{cf} &= \omega C_f V^{ref}_l e^{j90^0} \\ I^{ref}_{cd} &= \omega C_d V^{ref}_{sd} e^{j90^0} \end{aligned}\right\} \qquad (8)$$

In the (8) β is the scalar that defines how much reactive power must be supplied by the shunt compensator and q_{lav} is the average of the instantaneous load reactive power. If β=1, then the shunt active filter supplies entire reactive power required for the load i.e., the UPQC is operated in UPQC-Q mode. The transformation matrix M, is given below

$$M = \frac{1}{\sqrt{3}}\begin{bmatrix} 1 & 1 & 1 \\ 1 & e^{j240^0} & e^{j120^0} \\ 1 & e^{j120^0} & e^{j240^0} \end{bmatrix}$$

Note that the reference quantities obtained above are in phasor domain. These are then converted into instantaneous domain with respect to zero crossing of phase-a reference voltage phasor. These are tracked using the state feedback law of (7).

When the source voltages and load currents are unbalance and distorted, the terminal voltage and load current have the fundamental and harmonic components. Therefore, the load current and load voltage can be written as,

$$i_l = i_l^{fund} + i_l^{har}\ ;\ v_l = v_l^{fund} + v_l^{har} \qquad (9)$$

Where the subscripts *fund* and *har* denotes the fundamental and harmonic components respectively. The shunt filter must cancel out the harmonic content of the load current, therefore we get

$$i_f^{ref} = i_f^{fund} + i_l^{har} \quad (10)$$

Where i_f^{fund} is generated by using (10)

In the similar way, the reference for v_{sd} is given by

$$v_{sd}^{ref} = v_{sd}^{fund} - v_t^{har} \quad (11)$$

Where v_{sd}^{ref} is generated using (11)

The actual vector z is obtained by measuring $i_f, i_{cf}, v_l, i_{cd}, v_{sd}, i_l$ quantities in the system. Once the reference and actual vectors are obtained, the control signal *(u)* is obtained by using the appropriate control gain *(K)*.This is illustrated in Fig 4 and explained as follows.

After initial transient is over, the control is based only on the sign of the feedback controller and the output value of the feedback controller will chatter at a rate limited by the maximum switching frequency of the power switches. To avoid this, the hysteresis switching logic is used as given below

$$\left.\begin{array}{l}(u_{c1} \quad u_{c2})^T = u_c = -K\{z - z_{ref}\} \\ (u_1 \quad u_2)^T = u = hys\{z - z_{ref}\}\end{array}\right\} \quad (12)$$

If $h > lim$ then $hsy(h) = -1$

(in case of phase-a series inverter $\overline{s_{a1}}$=1 and $\overline{s_{a2}}$=1)

If $h < lim$ then $hsy(h) = 1$

(in case of phase-a series inverter s_{a1}=1 and s_{a2}=1)

In this the *"hys"* function is defined for a small limit *(lim)* around zero and h=K(z-z_{ref}).

The switching command $s_{a1}, \overline{s_{a1}}, s_{a2}$ and $\overline{s_{a2}}$ are shown in Fig.1. The switching signal $\overline{s_{a1}}$ is the complementary signal to s_{a1} and the same is true for other switches in different legs. In the same fashion, the switching logic has been obtained for other phases in the series and shunt inverter. Once u_{c1} and u_{c2} are computed, the switching functions u_1 and u_2 are obtained by (12). The reference signals are tracked by the shunt and series voltage source inverters of the UPQC to compensate the system. However, the most generally used LQR [5], [10], [14] method has some disadvantages over the proposed one, which are discussed in the next section.

V. LQR-BASED FEEDBACK CONTROLLER AND ITS SETBACKS

In the LQR method, in order to find the feedback gain K, a performance index J is chosen as

$$J = \int_0^\infty \{(Z - Z_{ref})^\Gamma Q(Z - Z_{ref}) + u_c^\Gamma R u_c\} dt \quad (13)$$

Where Q and R is the state vector and input vector weighing matrices. The weighing matrices Q and R are positive semi-definite respectively. Q and R weighing matrices set relative weights of state deviation and input usage respectively. The performance index J is minimized to obtain the optimal control law by solving Algebraic Riccati Equation (ARE). Parameters of the system shown in Fig. 3 are given in Table I. all of the parameters are in per unit. The base kilovolt amperes and base voltage are 5 kVA and 230 V, respectively. The weighing matrices for the LQR based feedback controller are chosen as Q=*diag*(20 1 10 1 10 0) and $R = (0.1 \quad 0.1)$, where *"diag"* is a diagonal matrix. Here, since the injected filter quantities are the important states to be controlled, highest priority is given to the states by giving higher weights to the corresponding elements in *Q*. Equal importance is given to both the series and shunt in the input weighing matrix. The feedback gain found by using LQR is

$$K = \begin{bmatrix} 7.339 & 4.8205 & 11.8275 & 0 & 0 & 0 \\ 0 & 0 & 0 & 3.3888 & 11.6077 & 0 \end{bmatrix}$$

The feeder and the load impedances are not fixed and may vary with considerable uncertainties. In fact the load impedances changes from instant to instant. Due to change in the feeder or load impedance, the state and input matrices A, B_1 also change with time. In other words these matrices involve parametric uncertainties. Even though the input matrix B_2 is constant, the control input (harmonic load current) is not fixed. The harmonic load current may vary with time. Since the feedback control law given in (7) is for the system at a particular operating condition with predefined harmonic content, it may not be able to give satisfactory operation under other operating conditions and parametric uncertainties. This may adversely affect the performance of the shunt and series compensation scheme. Another disadvantage is that the weighing matrices Q and R used for computing the feedback gain have to be chosen by a trial and error method. This type of search may or may not give optimal solution. In order to avoid these setbacks, in this work the feedback controller gains are tuned by optimization to give an optimal performance in various operating conditions with parametric uncertainties. In this paper Particle Swarm Optimization (PSO) has been used to find the feedback gain matrix K which can lead to optimal performance under parametric variations and system uncertainties. Particle swarm optimization (PSO) has been used as the optimization tool for solving power system stabilizer problems [16]–[18]. The PSO algorithm has been explained in the following sections

VI. PARTICLE SWARM OPTIMIZATION

Many areas in power systems require solving one or more nonlinear optimization problems. While analytical methods might suffer from slow convergence because of high dimensionality, heuristics-based swarm intelligence can be an efficient alternative. PSO, a part of the swarm intelligence family, is known to effectively solve large-scale nonlinear optimization problems[18]. PSO was familiarized in 1995 by Kennedy and Eberhart[19], which was inspired by the social behaviour of fish schooling and bird flocking. The PSO provides a population-based search process in which each individual called particles change their positions (states) with time. The PSO adopts "velocity-position" searching models. Each particle signifies a potential solution to a problem in D-dimensional space, whose superior or inferior degree can be evaluated by calculating its fitness. PSO is set with a group of random particles (solutions) and then exams for optimal values by updating generations. In each iteration, every particle is updated by following two "best" values. The first best solution (fitness) it has attained so far. This value is called pbest. Another "best" value that is tracked by the particle swarm optimizer is the best value, obtained so far by any particle in the population. This best value is a global best and called gbest. After finding the two best values, the particle updates its velocity and positions with following equation.

$$V_i^{n+1} = \omega V_i^n + c_1 r_1 (P_i^n - X_i^n) + c_2 r_2 (G_i^n - X_i^n) \quad (14)$$

$$X_i^{n+1} = X_i^n + V_i^{n+1} \quad (15)$$

where w is called the inertia weight; coefficients $c_1 c_2$ can have values between 1 to 2 and are called the study factors; r_1 and r_2 are random numbers between 0 and 1. This iterative process continues until the difference in the positions in successive iterations is below a predefined value. The inertia weight is employed to control the impact of the previous history of velocities on the current velocity. Thus, the parameter w regulates the tradeoff between the global and the local exploration abilities of the particle. The values for w are chosen empirically between 0.4 and 0.9 [20]-[21].

Compared by the genetic algorithm, the improvement in PSO that is it is very modest in terms of mathematical expression and understanding. Further, the PSO algorithm is faster in converging to a solution when compared to genetic algorithms (GAs) because of its mathematical simplicity. Due to the aforementioned advantages, the PSO-based technique has been used for UPQC.

VII. PSO-BASED FEEDBACK CONTROLLER OF UPQC

The PSO technique as explained above can be utilizes to design the state feedback controller of the UPQC. An optimization function can be developed to find the optimal feedback gains to maximize the left shift and increase the damping ratio of the Eigen values of the state matrix $\boldsymbol{\Lambda}$. The optimization function is given below.

$$\min f = \sum_{i=1}^{N} [\mathrm{Re}\{\lambda_i(\Lambda_i - \Gamma_{1i}K) + \lambda_{i\,\min\,\xi}(\Lambda_i - \Gamma_{1i}K)\}] \quad (16)$$

Subjected to

$$K_{\min 1} < K_1 < K_{\max 1},; K_{\min 2} < K_2 < K_{\max 2}; K_{\min 3} < K_3 < K_{\max 3}$$
$$K_{\min 4} < K_4 < K_{\max 4}; K_{\min 5} < K_5 < K_{\max 5}$$

Where $K = \begin{bmatrix} K_1 & K_2 & K_3 & 0 & 0 & 0 \\ 0 & 0 & 0 & K_4 & K_5 & 0 \end{bmatrix}$ and N is the number of possible operating conditions. K is the feedback controller gain vector having five non-zero elements. The terms Λ_i and Γ_{1i} represent the state and input matrices of the system at the 'i' operating condition respectively. It is not possible to find the load current reference, so partial feedback is considered. Similarly, the feedback is decoupled in order to avoid the effect of shunt filter action over the series filter action and vice versa. Hence, only five feedback gains have been used. The term $\lambda_{i\,\min\,\xi}$ represents the Eigen values corresponding to the least value of damping ratio (ξ) in case it is less than 1. Where ξ = 1 for all the Eigen values, this term contributes to zero. The term λ_i in represents the Eigen value with maximum real part. For practical reasons like limited switching frequency, the values of the K are limited.

TABLE I
SYSTEM PARAMETERS

System Parameters	Values
System voltage	1 p.u.
Loads	Zla=2+j1.5 p.u., Zlb=2.55+j1.25 p.u., and Zlc=1+j2.3 p.u.,
DC capacitors	2.5 p.u.
Feeder impedance	Zs=0.5+j0.3 p.u.,
UPQC parameters	Xcf=7.02 p.u., Xf=0.2 p.u., Rf=0 p.u., Xcd=4.0 p.u., Xd=0.04 p.u., Xt=0.1 p.u., and Rd=0 p.u.,

For the PSO based feedback controller, a linear decreasing inertia weight (χ) has been considered, starting from 0.9 and ending at 0.4. The cognitive and social inertia constant (C_1, C_2) are taken as 1.49. In the PSO implementation 50 particles and 100 iterations have been considered. The parameters of the proposed UPQC system are given in Table 1. By using (14) and (15), the feedback gains are found and are given by

$$K = \begin{bmatrix} 13.6759 & 6.5009 & 20 & 0 & 0 & 0 \\ 0 & 0 & 0 & 1.5219 & 14.0233 & 0 \end{bmatrix}$$

The PSO based design does have the disadvantage of sub-optimal performance of state feedback controller with partial feedback because the PSO tries to maximize the left shift of Eigen values directly with partial feedback. Also, it can be observed that with the state feedback controller design using PSO, the left shift of the critical eigenvalue is almost 3 times the value obtained by the ordinary LQR, hence ensuring more stability

VIII. SIMULATION RESULTS

The system parameters for the state feedback controller of the UPQC are the same as given in Table I. In addition to the R-L load, the three-phase rectifier load drawing an output current of 0.5 p.u. is also considered. The voltage of the dc capacitor C_{dc} shown in Fig. 2 is assumed to be constant as only steady state is considered. Various cases of parameter uncertainties are considered, and the performance of the control algorithm is presented in the following sections.

Case 1: Load and Feeder Impedances Are 100% (Base Case): Exactly, the source voltages are in per unit and represented as follows:

$$\left.\begin{aligned} v_{sa} &= \sqrt{2}\,\{\sin(\omega t) + (1/25)\sin(3\omega t) + (1/5)\sin(5\omega t) + (1/7)\sin(7\omega t)\} \\ v_{sb} &= 1.2\times\sqrt{2}\,\{\sin(\omega t - 120^0) + (1/25)\sin(3(\omega t - 120^0)) \\ &\quad + (1/5)\sin(5(\omega t - 120^0)) + (1/7)\sin(7(\omega t - 120^0))\} \\ v_{sc} &= 0.85\times\sqrt{2}\,\{\sin(\omega t + 120^0) + (1/25)\sin(3(\omega t + 120^0)) \\ &\quad + (1/5)\sin(5(\omega t + 120^0)) + (1/7)\sin(7(\omega t + 120^0))\} \end{aligned}\right\} \quad (18)$$

The harmonics in the source currents and terminal voltages are reduced when UPQC is provided with state feedback control de-signed either by the LQR or the PSO. It is mentioned here that the state feedback gain matrix $\boldsymbol{K}$ is computed for phase-a parameters. The same is used for the other two phases. The shunt filter currents with the PSO-based feedback controller are shown in Fig. 6(a) and similarly, the series filter voltages are shown in Fig. 6(b).

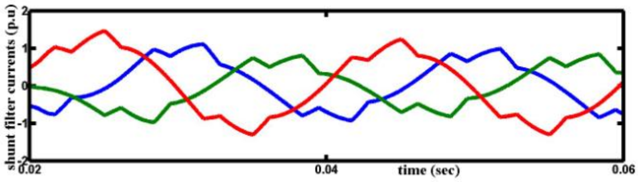

(a)

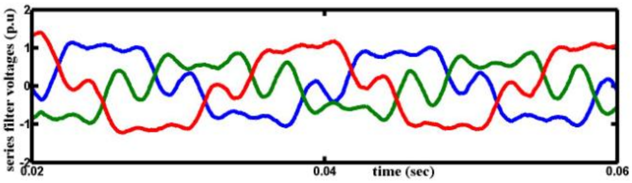

(b)

Fig. 6. Simulation results of Shunt filter currents and Series filter voltages.

The source voltage is unbalanced and distorted as shown in Fig. 7(a). The terminal voltages without any compensation are plotted in Fig. 7(b). It is observed that the terminal voltages contain notches due to the rectifier load. The corresponding load cur-rents are shown in Fig. 7(c).

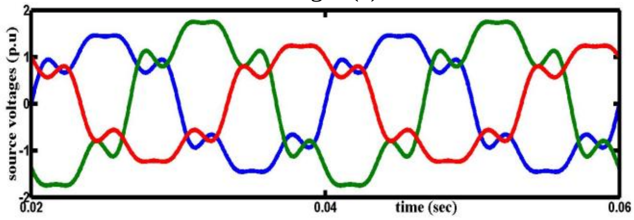

(a)

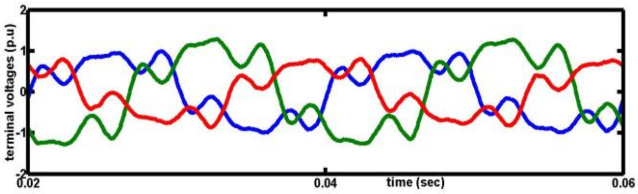

(b)

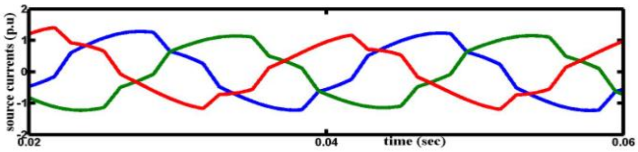

(c)

Fig. 7. Simulation result without any compensation.

The source currents and load voltages after compensation with LQR are shown in Fig. 8(a) and (b), respectively. The source currents and load voltages after compensation with PSO are shown in Fig. 8(c) and (d), respectively.

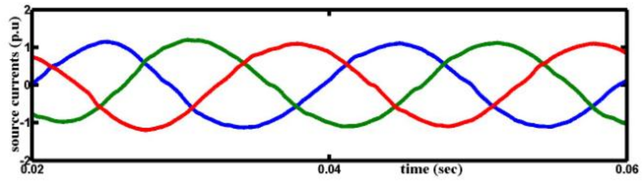

(a)

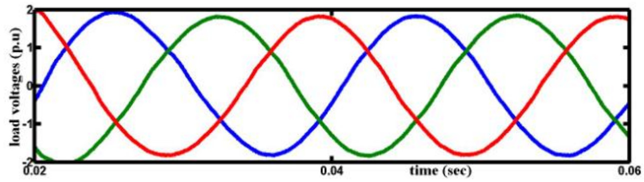

(b)

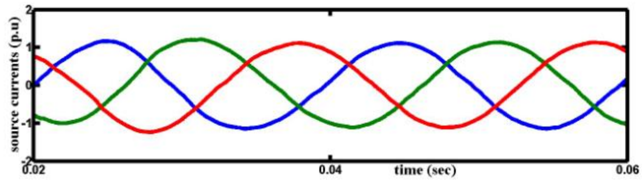

(c)

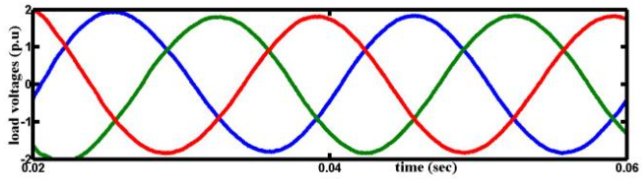

(d)

Fig. 8. Simulation results after compensation with ordinary LQR and PSO

THDs of source current and load voltage with the LQR-based state feedback controller are 2.8% and 1.2% in phase-a, whereas with the PSO-based state feedback controller, the THDs are just 1.3% and 0.5%, respectively. The performance of the PSO-based feedback controller in terms of reducing the THD of source currents and load voltages is better than the LQR-based feedback controller

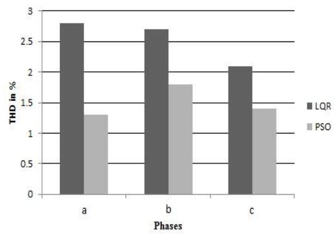

(a)

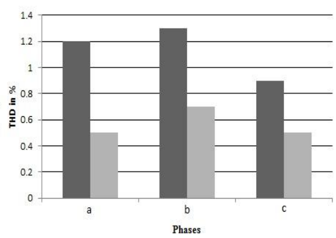

(b)

Fig. 9 (a) Source current THD (b) Load voltage THD

Case 2: Load Impedances Are Increased by 100%: From the base case the load impedance is increased by 100% without any change in other parameters of the system. The load voltage and source current after compensation with LQR and PSO are shown in Fig.10.

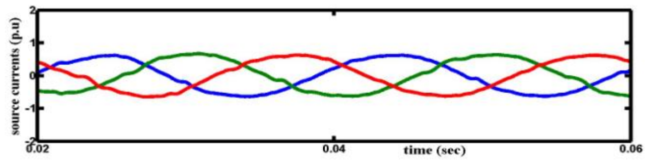

(a)

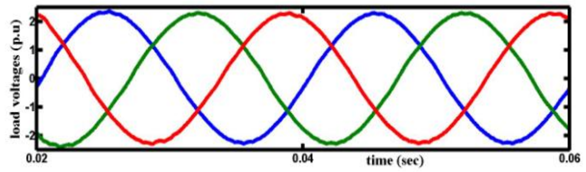

(b)

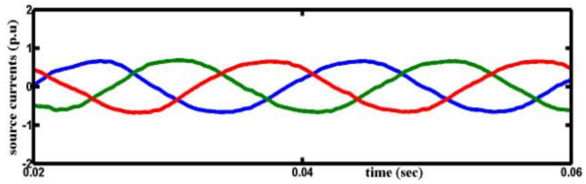

(c)

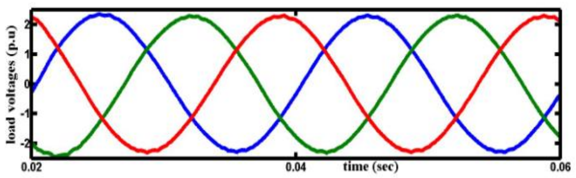

(d)

Fig. 10 (a) Source currents after compensation with the LQR. (b) Load voltages after compensation with the LQR. (c) Source currents after compensation with the PSO. (d) Load voltages after compensation with the PSO.

THD of source current and load voltage with LQR and PSO are shown in Fig.11. If there is any change in operating condition, the gain calculated by LQR method cannot be optimum. The PSO works well for the uncertain parametric changes due its advantages.

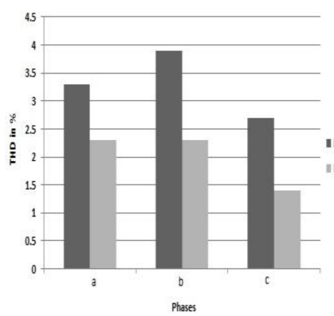

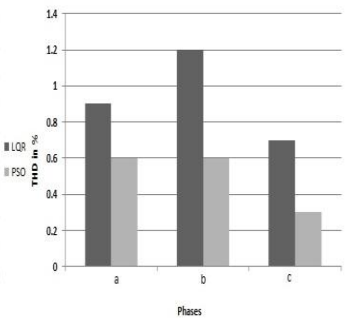

(a) (b)

Fig. 11 (a) Source current THD (b) Load voltage THD

TABLE II
THD OF THE SOURCE CURRENT WITH STATEFEEDBACK CONTROLLER

THD %	Without compensation		Case 1		Case 2	
	Case 1	Case 2	LQR	PSO	LQR	PSO
i_{sa}	9.7	10.4	2.8	1.3	3.3	2.3
i_{sb}	10.0	13.1	2.7	1.8	3.9	2.3
i_{sc}	11.1	14.5	2.1	1.4	2.7	1.4

TABLE III
THD OF THE LOAD VOLTAGE WITH STATEFEEDBACK CONTROLLER

THD %	Without compensation		Case 1		Case 2	
	Case 1	Case 2	LQR	PSO	LQR	PSO
v_{ta}	3.4	3.6	1.2	0.5	0.9	0.6
v_{tb}	3.6	3.7	1.3	0.7	1.2	0.6
v_{tc}	3.3	3.5	0.9	0.5	0.7	0.3

IX. CONCLUSION

The state feedback controller of UPQC has been designed by two different methodologies i.e., the LQR and the PSO. The PSO based state feedback controller has several advantages over the LQR as latter involves trial and error process for deciding the parameter values like **Q** and **R.** Unlike LQR based feedback controller, PSO based feedback controller does not have a sub-optimal performance in the case of partial state feedback. It has been observed from the simulation results that the state feedback controller designed using PSO has better performance in terms of reducing the THD of source currents and load voltages when compared to the state feedback controller designed by the LQR. The robustness of the PSO based feedback controller has been verified by considering the performance in various operating conditions. It was observed that in all the operating conditions proposed PSO based controller outperformed the LQR based feedback controller under distorted supply voltages.

REFERENCES

[1] F. Z. Peng and J. S. Lai, "Generalized instantaneous reactive power theory for three-phase power systems," *IEEE Trans. Instrum. Meas.*, vol. 45, no. 1, pp. 293–297, Feb. 1996.

[2] A. Ghosh, A. K. Jindal, and A. Joshi, "Design of a capacitor-supported dynamic voltage restorer (DVR) for unbalanced and distorted loads," *IEEE Trans. Power Del.*, vol. 19, no. 1, pp. 405–413, Jan. 2004

[3] N. H. Woodley, L. Morgan, and A. Sundaram, "Experience with an inverter-based dynamic voltage restorer," *IEEE Trans. Power Del.*, vol. 14, no. 3, pp. 1181–1186, Jul. 1999. .

[4] H. Akagi, Y. Kanazawa, and A. Nabae, "Instantaneous reactive power compensators comprising switching devices without energy storage components," *IEEE Trans. Ind. Appl.*, vol. IA-20, no. 3, pp. 625–630, May 1984.

[5] A. Ghosh and G. Ledwich, "A unified power quality conditioner (UPQC) for simultaneous voltage and current compensation," *Elect. Power Syst. Res.*, vol. 59, no. 1, pp. 55–63, Aug. 2001.

[6] A. Ghosh and A. Joshi, "A new approach to load balancing and power factor correction in power distribution system," *IEEE Trans. Power Del.*, vol. 15, no. 1, pp. 417–422, Jan. 2000.

[7] H. Fujita and H. Akagi, "The unified power quality conditioner: The integration of series active filters and shunt active filters," *IEEE Trans. Power Electron.*, vol. 13, no. 2, pp. 315–322, Mar. 1998.

[8] M. Basu, S. P. Das, and G. K. Dubey, "Comparative evaluation of two models of UPQC for suitable interface to enhance power quality," *Elect. Power Syst. Res.*, vol. 77, no. 7, pp. 821–830, May 2007.

[9] M. R. Banaei, S. H. Hosseini, S. Khanmohamadi, and G. B. Ghareh-petian, "Loss reduction of distribution system using APLC," *Elect. Power Syst. Res.*, vol. 13, no. 2, pp. 169–178, Feb. 2005.

[10] Y. Rong, C. Li, H. Tang, and X. Zheng, "Output feedback control of single-phase UPQC based on novel model," *IEEE Trans. Power Del.*, vol. 24, no. 3, pp. 1586–1597, Jul. 2009.

[11] V. George and M. K. Mishra, "DSTATCOM topologies for three—Phase high power applications," *Int. J. Power Electron.*, vol. 2, no. 2, pp. 107–124, 2010.

[12] A. Ghosh and G. Ledwich, *Power Quality Enhancement Using Custom Power Devices*. Norwell, MA: Kluwer, 2002.

[13] W. A. Lyon, *Transient Analysis of Alternating-Current Machinery*. New York: Wiley, 1954, ch. 2.

[14] B. Kedjar and K. Al-Haddad, "DSP-based implementation of an LQR with integral action for three-phase three-wire shunt active power filter," *IEEE Trans. Ind. Electron.*, vol. 56, no. 8, pp. 2812–2828, Aug. 2009.

[15] B. D. O. Anderson and J. B. Moore, *Linear Optimal Control*. Engle-wood Cliffs, NJ: Prentice-Hall, 1971.

[16] A. T. Al-Awami, Y. L. Abdel-Magid, and M. A. Abido, "A particle-swarm-based approach of power system stability enhancement with unified power flow controller," *Int. J. Elect. Power Energy Syst.*, vol. 29, no. 3, pp. 251–259, Mar. 2007.

[17] S. Panda and N. P. Padhy, "Optimal location and controller design of STATCOM for power system stability improvement using PSO," *J. Franklin Inst.*, vol. 345, no. 2, pp. 166–181, Mar. 2008.

[18] G. Coath, M. Al-Dabbagh, and S. K. Halgamuge, "A comparison of constraint-handling methods for the application of particle swarm op-timization to constrained nonlinear optimization problems," in *Proc. IEEE Power Eng. Soc. General Meeting*, Jun. 6–10, 2004, pp. 303–308.

[19] J. Kennedy and R. Eberhart, "Particle swarm optimization," presented at the IEEE Int. Conf. Neural Networks, Perth, Australia.

[20] Y. Shi and R. C. Eberhart, "Empirical study of particle swarm opti-mization," in *Proc. Congr. Evolutionary Computation*, Jul. 6–9, 1999, vol. 3, pp. 1945–1950.

[21] Y. del valle *et al.*, "Particle swarm optimization: Basic concepts vari-ants and applications in power systems," *IEEE Trans. Evol. Comput.*, vol. 12, no. 2, pp. 171–195, Apr. 2008.

[22] S. Panda and N. P. Padhy, "Comparison of particle swarm optimization and genetic algorithm for FACTS-based controller design," *Appl. Soft Comput.*, vol. 8, no. 4, pp. 1418–1427, Sep. 2008.

[23] N.G.Hingorani, "Introducing Custom Power", IEEE Spectrum. Vol.32.pp.41-48.95

[24] R. C. Eberhart and Y. Shi, "Comparison between genetic algorithm and particle swarm optimization," in *Proc. 7th Annu. Conf. Evolutionary Programming*, San Diego, CA, 1998, pp. 611–616